Human Molecular Genetics, 2014 **1–10**
doi:10.1093/hmg/ddu329

S81L and G170R mutations causing Primary Hyperoxaluria type I in homozygosis and heterozygosis: an example of positive interallelic complementation

Riccardo Montioli[1,†], Alessandro Roncador[1,†], Elisa Oppici[1], Giorgia Mandrile[2], Daniela Francesca Giachino[2], Barbara Cellini[1,*] and Carla Borri Voltattorni[1]

[1]Department of Life Sciences and Reproduction, University of Verona, Verona, Italy and [2]Department of Clinical and Biological Sciences, University of Torino, Torino, Italy

Received May 20, 2014; Revised and Accepted June 20, 2014

Primary Hyperoxaluria type I (PH1) is a rare disease due to the deficit of peroxisomal alanine:glyoxylate aminotransferase (AGT), a homodimeric pyridoxal-5′-phosphate (PLP) enzyme present in humans as major (Ma) and minor (Mi) allele. PH1-causing mutations are mostly missense identified in both homozygous and compound heterozygous patients. Until now, the pathogenesis of PH1 has been only studied by approaches mimicking homozygous patients, whereas the molecular aspects of the genotype-enzymatic-clinical phenotype relationship in compound heterozygous patients are completely unknown. Here, for the first time, we elucidate the enzymatic phenotype linked to the S81L mutation on AGT-Ma, relative to a PLP-binding residue, and how it changes when the most common mutation G170R on AGT-Mi, known to cause AGT mistargeting without affecting the enzyme functionality, is present in the second allele. By using a bicistronic eukaryotic expression vector, we demonstrate that (i) S81L-Ma is mainly in its apo-form and has a significant peroxisomal localization and (ii) S81L and G170R monomers interact giving rise to the G170R-Mi/S81L-Ma holo-form, which is imported into peroxisomes and exhibits an enhanced functionality with respect to the parental enzymes. These data, integrated with the biochemical features of the heterodimer and the homodimeric counterparts in their purified recombinant form, (i) highlight the molecular basis of the pathogenicity of S81L-Ma and (ii) provide evidence for a positive interallelic complementation between the S81L and G170R monomers. Our study represents a valid approach to investigate the molecular pathogenesis of PH1 in compound heterozygous patients.

INTRODUCTION

Liver peroxisomal alanine:glyoxylate aminotransferase (AGT) is a homodimeric pyridoxal-5′-phosphate (PLP)-dependent enzyme, which catalyses the conversion of L-alanine and glyoxylate to pyruvate and glycine, respectively. AGT deficiency is responsible for Primary Hyperoxaluria type I (PH1) (MIM 259900), a rare autosomal recessive disease with an estimated prevalence of 1–3 per million population in Europe (1,2). In PH1 patients, glyoxylate accumulation and its conversion to the metabolic end product oxalate lead to calcium oxalate (CaOx) supersaturation and precipitation as CaOx stones. This condition manifests as urolithiasis and/or nephrocalcinosis, and, if untreated, as systemic oxalosis with CaOx deposition in many organs (3).

The *AGXT* gene encoding AGT is present in human population as two haplotypes, the 'major' (encoding AGT-Ma) and the 'minor' (encoding AGT-Mi), the latter characterized by a 74-bp duplication in intron 1 and two point mutations causing the P11L and I340M amino acid substitutions (4). Most of the mutations associated with PH1 (>150) are missense and

*To whom correspondence should be addressed at: Department of Life Sciences and Reproduction, Section of Biological Chemistry, University of Verona, Strada Le Grazie, 8, Verona, Italy. Tel: +39 0458027293; Fax: +39 0458027170; Email: barbara.cellini@univr.it
†The authors wish it to be known that, in their opinion, the first two authors should be regarded as joint First Authors.

concern residues spread over the entire 3D structure of the enzyme (5). Biochemical, bioinformatic and cell biology studies have revealed that pathogenic mutations can either alter the AGT catalytic machinery (6–9) and/or undermine the stability of the folded conformation (10–14) leading, in most cases, to protein aggregation and/or mitochondrial mistargeting (15). Moreover, some mutations have only an impact on the apo-form of the protein (12,16,17).

Like in other recessive diseases, a substantial share of PH1 patients are compound heterozygous expressing two different AGT alleles. In these patients, interallelic complementation (IC) phenomena could occur, leading to a phenotype less severe (positive IC) or a more severe (negative IC) than that of the homozygous counterparts. Interallelic complementation effects arise from the combination of monomers bearing different mutations yielding heterodimeric species with functional and/or structural properties different from the average of those of parental homodimers. Until now, only 'single protein' studies have been undertaken to investigate the molecular pathogenesis of PH1, and the possible interplay between two different pathogenic mutations at clinical and enzyme level has never been analysed. Taking into account that many PH1 patients are compound heterozygous, the investigation of their heterozygous status is highly desirable and will possibly further expand the phenotype spectrum of the disease.

Here, we started from the clinical data on two PH1 patients, one hemizygous for the S81L mutation associated with the major allele and the other compound heterozygous for the S81L mutation on the major allele and the most common mutation in Caucasian patients, i.e. the G170R associated with the minor allele. It is known that the G170R mutation does not affect the kinetic and coenzyme binding properties of AGT (17) but causes a folding defect leading to an erroneous targeting to mitochondria, where the enzyme cannot perform glyoxylate detoxification (18). The S81L pathogenic mutation has been firstly identified by Williams *et al*. (19). Ser81 forms a hydrogen bond with the phosphate group of PLP and, although the molecular defect of the S81L-Ma variant is unknown, the mutation to Leu has been predicted to mainly affect the coenzyme binding affinity (20). We used a bicistronic eukaryotic expression vector and a dual-vector prokaryotic expression strategy to study for the first time not only the consequences of the S81L mutation on AGT but also the interplay at molecular and cellular level between the G170R and the S81L mutations. By investigating the effects of each mutation and those of their combination on the expression level, specific activity, subcellular localization, functionality as well as on the coenzyme binding affinity and the kinetic and spectroscopic properties of AGT, we were able to (i) elucidate the molecular defects of the S81L-Ma variant, (ii) mimic in mammalian cells the natural heteroallelic state occurring in compound heterozygous patients bearing the S81L and the G170R mutations, (iii) isolate and characterize the G170R-Mi/S81L-Ma heterodimer and (iv) provide evidence for a global positive IC effect between the G170R and S81L mutations.

RESULTS

Clinical cases

Patient 1 is a 30-year-old Albanian male, affected by nephrolithiasis since age 3. PH1 was diagnosed at age 24 (AGT activity in liver biopsy reduced to 23% of normal). At diagnosis, urography showed atrophy of the right kidney and multiple stones in the left one. Serum creatinin was 1.18 mg/dl, creatinin clearance 86 ml/min/1.73 mq, urinary oxalate 1.3 mmol/24 h, urinary glycolate 830 μmol/24 h, plasma oxalate 8 μmol/l and plasma glycolate 5 μmol/l. He had a good pyridoxine response (600 mg/die): urinary oxalate decreased to 0.480 mmol/24 h and plasma oxalate to 0.8 μmol/l. At age 32, serum creatinin was 1.5 mg/dl and urinary oxalate 0.35 mmol/die; no systemic oxalosis was present. *AGXT* gene sequencing demonstrated compound heterozygosis for S81L and G170R mutations (on major and minor haplotype, respectively). No kidney disease was reported in the family, nor consanguinity among parents.

Patient 2 is a 15-year-old Serbian female; at 11 months, she presented failure to thrive, anorexia and recurrent kidney stones; at that time, urinary oxalate was 242 mmol/24 h. End-stage renal disease (ESRD) occurred at age 11 (serum creatinin 1744 μmol/l). Plasma oxalate was 110 μmol/l. At that time, abdominal ultrasound showed nephrocalcinosis and kidney volume reduction. She presented growth retardation (height: $<10^{\circ}$ centile; weight: $3-10^{\circ}$ centile), painful bone attacks and leg deformity (genu varum) owing to systemic oxalosis. At age 15, she developed hyperparathyroidism, mild left ventricular hypertrophy and heart dilatation and non-specific central irritation at electroencephalogram (no seizures referred). No formal pyridoxine testing was performed. She underwent a combined kidney–liver transplant at age 15. *AGXT* gene sequencing demonstrated compound heterozygosis for S81L and S205X mutations (both on major haplotype). Thus, this patient can be considered 'functionally hemizygous' for the non-null mutation, because it only expresses the allele bearing the S81L mutation. No kidney disease was reported in the family, nor consanguinity among parents.

Based on these data, which indicate a different severity of the two cases, we decided to investigate the enzymatic phenotype associated with the S81L mutation on the major allele as well as the occurrence of possible IC effects between the S81L and the G170R mutation on the minor allele. To this aim, considering the great variety of the molecular mechanisms leading to AGT deficiency in PH1, we studied the consequences of each mutation alone and of their combination on (i) the protein expression level, the specific activity, the subcellular localization and the functionality upon expression in a eukaryotic cellular system and (ii) the coenzyme binding affinity and the spectroscopic and kinetic features of purified variants in the homodimeric and heterodimeric state.

S81L and G170R mutations in homozygous and heterozygous conditions: effect on the expression level and the specific activity of AGT

We investigated the cellular effects of the S81L mutation on AGT-Ma both in conditions mimicking a homozygous patient and in conditions mimicking a compound heterozygous patient bearing the G170R mutation on AGT-Mi in the second allele. To this aim, we constructed a series of pIRES vectors that allowed us to express under the same transcript two copies of the AGT cDNA bearing the analysed polymorphic and pathogenic mutations in different combinations (Fig. 1). To distinguish between the first and the second gene product, we

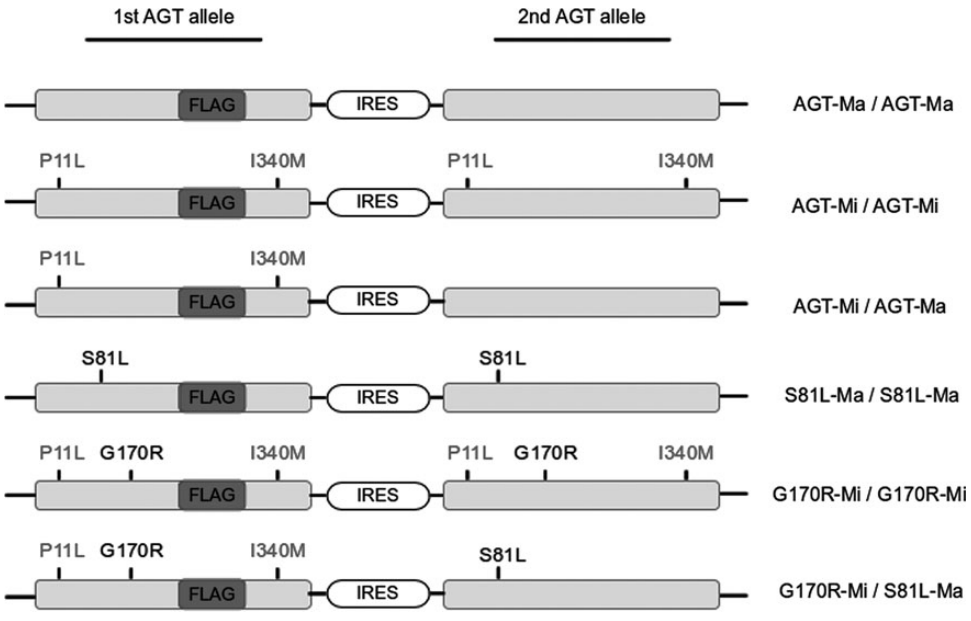

Figure 1. Graphical sketch of the bicistronic pIRES constructs expressing the AGT variants. The first ORF is bearing the FLAG sequence. Polymorphic and pathogenic mutations in each construct are marked grey and black, respectively.

introduced a FLAG tag on the surface portion of the loop 251–266, exactly between the residues 254 and 255 of the first gene product. The chosen site, away from both the C-terminal peroxisomal targeting sequence and the active site, is predicted to accommodate the tag without generating significant steric hindrance. As shown in Figure 1, in the constructs encoding two different enzymatic species, the FLAG tag was inserted on the background of the minor allele. This allowed us to detect only the product of the second allele by an antibody specific for AGT-Ma. Each vector was transduced in CHO-GO cells, which stably express glycolate oxidase (GO) and represent a widely used cellular model for PH1 (21). Preliminary transient transfection experiments showed that the presence of the FLAG tag did not significantly affect the AGT expression level, the enzymatic activity and the intracellular trafficking. Thus, CHO-GO clones stably expressing each of the constructs were selected, and the levels of expressed AGT were analysed by western blot. A double band responsive to the anti-AGT antibody, absent in the parental cells, is present in all the clones (Fig. 2A and B). The band at the higher molecular weight is also responsive to the anti-FLAG antibody, thus confirming that the clones express both AGT alleles. To investigate whether the coexpression of the two allelic forms actually generates heterodimeric species, we immunoprecipitated stably transfected CHO-GO cells expressing AGT-Mi/AGT-Mi, G170R-Mi/G170R-Mi, AGT-Mi/AGT-Ma and G170R-Mi/S81L-Ma with an anti-FLAG antibody and we detected the precipitated proteins by western blot using an antibody specific for AGT-Ma (Fig. 3). The anti-FLAG antibody pulled down a protein that reacted with the anti-AGT-Ma antibody only in the AGT-Mi/AGT-Ma and G170R-Mi/S81L-Ma clones. This indicates the formation of heterodimeric species in these samples, because the FLAG tag is present on the first allele, whereas the AGT-Ma epitope in these constructs is encoded by the second allele (Fig. 1). These data validate our experimental model for the study of the S81L and G170R mutations in heterozygous state and the evaluation of possible IC effects at cellular level. However, these results should be interpreted with caution considering that the relative proportions of homodimeric and heterodimeric species cannot be measured under these experimental conditions.

In line with previous data (15), the expression level of AGT-Mi/AGT-Mi, AGT-Mi/AGT-Ma and G170R-Mi/G170R-Mi was about 75, 90 and 46%, respectively, that of AGT-Ma/AGT-Ma. Moreover, while the S81L mutation did not significantly reduce the expression level of AGT-Ma/AGT-Ma, cells expressing the G170R-Mi/S81L-Ma construct showed an AGT expression level equal to ∼30% that of cells expressing AGT-Mi/AGT-Ma (Fig. 2A and B). Similar results were obtained in different clones expressing the G170R-Mi/S81L-Ma construct, and real-time PCR experiments did not reveal differences between the clones at transcription level. Thus, the reduced AGT level in G170R-Mi/S81L-Ma transfectants should originate from a defect at the protein level leading to an increased aggregation and/or degradation propensity of the heterodimeric form with respect to the homodimers G170R-Mi and S81L-Ma. In this regard, we found that in cells expressing the G170R-Mi/S81L-Ma construct, (i) the ratio of soluble/insoluble AGT does not significantly differ from that of cells expressing the AGT-Mi/AGT-Ma construct, and (ii) no aggregates of AGT can be revealed upon cross-linking with bis-N-succinimidyl-(pentaethyleneglyocol) ester. Thus, it can be suggested that the low AGT expression level of the clone G170R-Mi/S81L-Ma could arise from an increased susceptibility to degradation of the heterodimeric species with respect to the homodimers G170R-Mi and S81L-Ma (see below).

We then measured the specific activity of each clone in the absence and presence of PLP in the assay mixture, representing the amount of the holoenzyme and of the total active protein (apoenzyme plus holoenzyme), respectively (Fig. 2C). In the

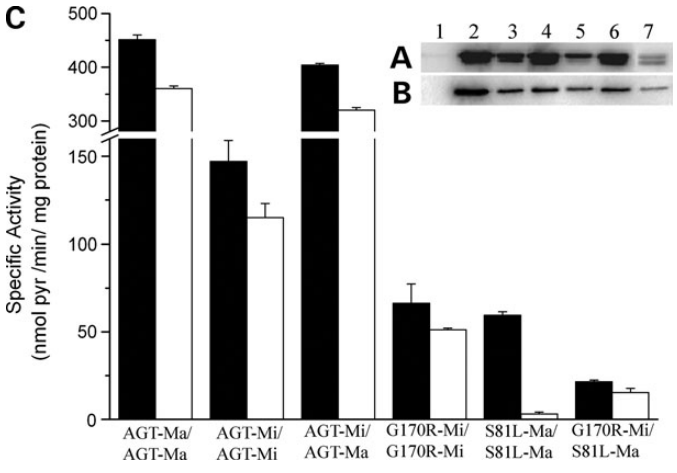

Figure 2. Western blot and specific activity analyses of CHO-GO cell clones expressing the AGT variants. Four micrograms of cell lysate was immunoblotted with (**A**) anti-AGT from rabbit and anti-rabbit HRP-conjugated antibodies and (**B**) mouse anti-FLAG and anti-mouse HRP-conjugated antibodies. Lanes: 1. CHO-GO; 2. AGT-Ma/AGT-Ma; 3. AGT-Mi/AGT-Mi; 4. AGT-Mi/AGT-Ma; 5. G170R-Mi/G170R-Mi; 6. S81L-Ma/S81L-Ma; 7. G170R-Mi/S81L-Ma. (**C**) Hundred micrograms of cell lysate were incubated with 0.5 M L-alanine and 10 mM glyoxylate at 25°C in 100 mM KP, pH 7.4, in the presence (black) or in the absence (white) of 200 μM PLP. Data are representative of three independent experiments. Bar graphs represent the mean ± SD.

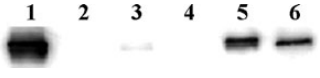

Figure 3. Identification of the presence of heterodimeric forms of AGT by immunoprecipitation. Three hundred micrograms of cell lysate were immunoprecipitated using an anti-FLAG antibody and detected by western blot using rabbit anti-AGT-Ma and anti-rabbit HRP-conjugated antibodies. Lanes: 1. purified AGT-Ma control non-immunoprecipitated; 2. CHO-GO parental cells; 3. AGT-Mi/AGT-Mi; 4. G170R-Mi/G170R-Mi; 5. AGT-Mi/AGT-Ma; 6. G170R-Mi/S81L-Ma.

presence of PLP, the specific activity of AGT-Mi/AGT-Mi and AGT-Mi/AGT-Ma was reduced by ∼35 and 20% with respect to that of AGT-Ma/AGT-Ma, whereas that of G170R-Mi/G170R-Mi is reduced by ∼70% with respect to that of AGT-Mi/AGT-Mi, in line with previous data on cellular lysates (15). Moreover, the specific activity of S81L-Ma/S81L-Ma was ∼20% that of AGT-Ma/AGT-Ma, whereas that of G170R-Mi/S81L-Ma was ∼4% that of AGT-Mi/AGT-Ma. As compared with the activity in the presence of added coenzyme, the specific activity of AGT-Ma/AGT-Ma, AGT-Mi/AGT-Mi, AGT-Mi/AGT-Ma and G170R-Mi/G170R-Mi measured in the absence of PLP decreased by 25–30% and that of G170R-Mi/S81L-Ma decreased by 40%, thus indicating that in these clones, AGT is in large amount present as holoenzyme. In contrast, the specific activity of S81L-Ma/S81L-Ma decreased by 95% in the absence of PLP in the assay mixture, thus revealing that this variant in the cell is almost entirely present as apoenzyme.

Overall, the data obtained in the CHO-GO cellular model indicate that (i) the S81L-Ma variant is almost entirely present as apoenzyme in the cell and its reduced specific activity is not ascribable to a reduced expression level and (ii) when the S81L-Ma and the G170R-Mi variants are co-expressed in the same cell, the formed heterodimeric species are mainly present as holoenzymes, but the total AGT expression level is lower than that of cells expressing homodimeric S81L-Ma or G170R-Mi.

Table 1. Kinetic parameters and $K_{D(PLP)}$ values of the AGT variants

Enzyme	$K_{D(PLP)}$ (μM)	k_{cat}/s^{-1}	$K_{m\ L\text{-}ala}$ (mM)	$K_{m\ glyoxylate}$ (mM)
AGT-Ma (6)	0.27 ± 0.03	45 ± 2	31 ± 4	0.23 ± 0.05
AGT-Mi (10)	0.26 ± 0.02	37 ± 5	28 ± 2	0.22 ± 0.01
G170R-Mi (17)	0.4 ± 0.1	34 ± 3	36 ± 2	0.4 ± 0.1
S81L-Ma	17 ± 3	13.9 ± 0.9	40 ± 8	0.16 ± 0.02
G170R-Mi/S81L-Ma	1.2 ± 0.1	18.3 ± 0.6	45 ± 3	0.18 ± 0.02

S81L and G170R mutations in homozygous and heterozygous conditions: effect on the structural and the functional properties of AGT

Although the data obtained in CHO-GO cells confirm the pathogenicity of the mutations, they do not allow the identification of the molecular mechanisms(s) by which the S81L mutation, both in homozygosis and in heterozygosis with the G170R mutation, generates the AGT malfunction. To gain insights into this issue, the homodimer S81L-Ma and the heterodimer G170R-Mi/S81L-Ma were expressed in *Escherichia coli*, purified and characterized. Their spectroscopic and kinetic properties were compared with those of AGT-Ma, AGT-Mi and G170R-Mi, previously studied (17). Absorbance, visible and near-UV CD spectra of S81L-Ma and G170R-Mi/S81L-Ma in the holo-form were similar to each other and to the corresponding ones of AGT-Ma, AGT-Mi and G170R-Mi. Nevertheless, while no significant changes were observed in 1-anilino naphthalene sulphonic acid (ANS) emission fluorescence for the holo-forms of AGT-Ma, AGT-Mi, S81L-Ma and G170R-Mi, an about 10-fold increase in ANS emission fluorescence intensity in the holo-heterodimer G170R-Mi/S81L-Ma was observed (Supplementary Material, Fig. S4). This indicates that the heterodimeric species displays an increased exposure of hydrophobic patches on its surface, thus suggesting that the formation of the heterodimer causes a conformational change with respect to the homodimeric species. Following this view, we can speculate that, as found for other proteins that fold in the cell cytosol (22), the increased exposure of hydrophobic surfaces would possibly induce the proteasomal degradation of the heterodimer by triggering the cellular quality control machinery.

The effect of the S81L mutation on the PLP binding affinity of the homodimer and the heterodimer was also investigated. As expected, considering that Ser81 is hydrogen-bonded with the PLP phosphate, the S81L-Ma homodimer displayed a ∼70-fold increase in the equilibrium dissociation constant for PLP ($K_{D(PLP)}$) with respect to AGT-Ma (Table 1). This explains why in CHO-GO cells expressing the S81L-Ma/S81L-Ma construct grown in a medium containing ∼0.3 μM pyridoxine [a concentration even higher than that present in human plasma (23)], the variant was almost completely present in the apo-form. Unexpectedly, the G170R-Mi/S81L-Ma heterodimer showed a $K_{D(PLP)}$ value ∼7-fold lower than that predicted by averaging the $K_{D(PLP)}$ values of the two parental enzymes (Table 1). In trying to explain this result, we modelled the

putative dimeric structure of AGT through a crystallographic symmetry operation on the available monomeric structure [pdb file 1H0C (5)]. It revealed that the phosphate group of PLP in each active site interacts with the Oβ of Ser81 and with the peptidic N(s) of Gly82 and His83 of the one's own subunit, and with the Oδ of Tyr260 and the peptidic N of Thr263 of the neighbouring subunit (Supplementary Material, Fig. S1A). The Ser81 → Leu substitution (i) eliminates the H bonds that stabilizes the PLP binding, (ii) introduces a bulky hydrophobic side chain in a polar region of the interface between the AGT monomers and (iii) generates a significant steric hindrance that could compromise the H-bond between His262 and Ser79 of the neighbouring subunit (Supplementary Material, Fig. S1B). This in turn can destabilize the loop 251–266 and the stretch 79–83 of the neighbouring subunit, both involved in PLP binding. On these bases, the S81L mutation is predicted to directly affect the cofactor binding to one subunit but also to indirectly perturb the PLP binding pocket of the adjacent subunit. The lack of this indirect effect in the heterodimer G170R-Mi/S81L-Ma may explain its PLP binding affinity higher than that expected.

The steady-state kinetic parameters reported in Table 1 show that the S81L-Ma homodimer was characterized by a 3-fold decrease in the k_{cat} value with respect to AGT-Ma, whereas the G170R-Mi/S81L-Ma heterodimer displayed a k_{cat} value slightly lower than that predicted by averaging the k_{cat} values of the homodimeric counterparts. There were no significant differences in the K_M values of the examined variants.

Taken together, these data provide evidence that (i) the S81L mutation mainly induces a functional defect, by reducing the AGT catalytic activity and strongly decreasing the coenzyme binding affinity and (ii) the heterodimer G170R-Mi/S81L-Ma shows k_{cat} and $K_{D(PLP)}$ values similar to or lower than, respectively, those derived by the average of the corresponding ones of the homodimeric counterparts.

S81L and G170R mutations in homozygous and heterozygous conditions: effect on the AGT subcellular localization

The G170R mutation on the minor allele is known to cause the mitochondrial mistargeting of AGT, owing to the synergism between the polymorphic P11L mutation, generating a putative mitochondrial targeting sequence (MTS), and the G170R mutation, which induces a folding defect on apodimeric AGT that results in the formation of monomeric folding intermediates prone to interact with molecular chaperons and compatible with the mitochondrial import (12,15,17,18,24,25). In fact, while peroxisomes can import fully folded oligomeric proteins, mitochondria import species bearing an MTS in partly folded monomeric conformation. Up to date, no information is available on the effect of the S81L mutation in homozygosis and heterozygosis with G170R on the AGT subcellular localization. Thus, the stable clones of CHO-GO cells expressing the various constructs were analysed by immunofluorescence microscopy (IFM) both qualitatively, by evaluating the RGB profile of the images, and quantitatively, by determining the Pearson coefficient of each sample (Figs 4, 5, Supplementary Material, Figs S2, S3 and 6). The Pearson coefficient can be used to estimate the colocalization between two signals evaluating the correlation between the signal

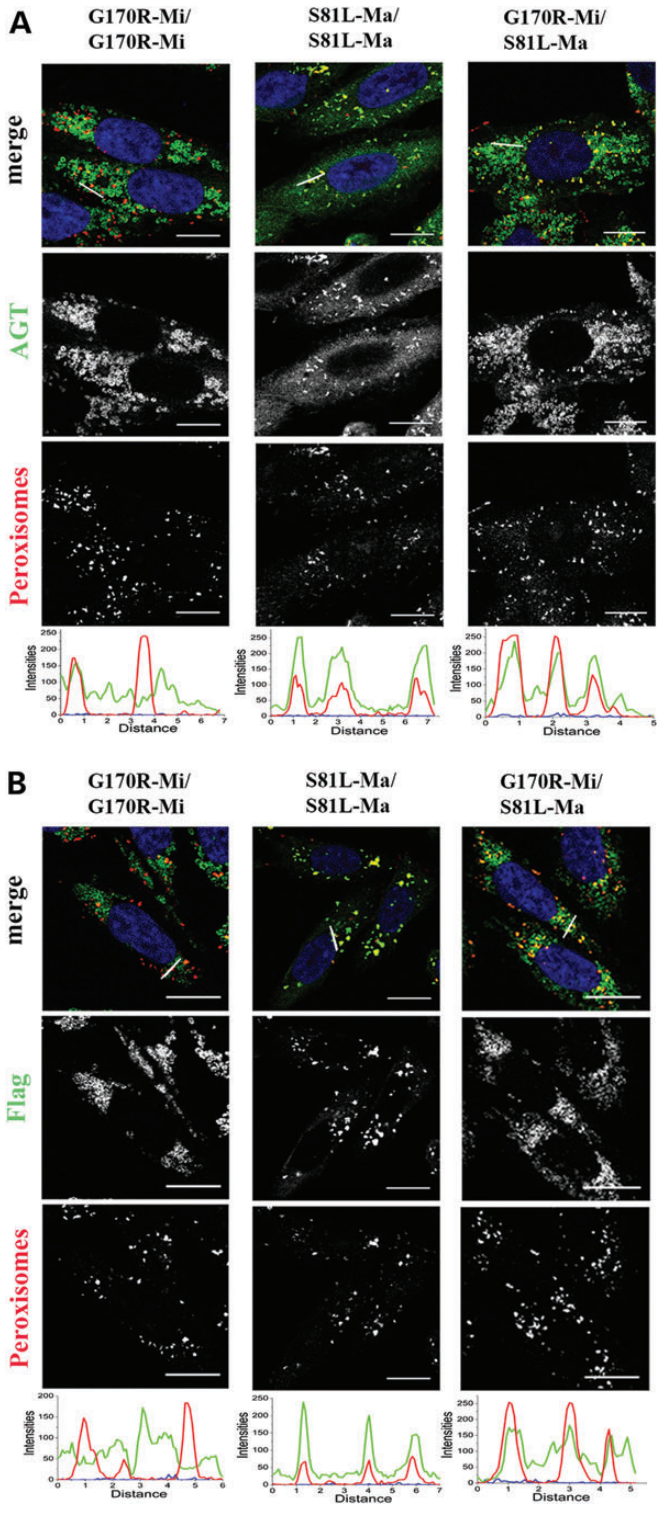

Figure 4. Subcellular distribution of G170R-Mi/G170R-Mi, S81L-Ma/S81L-Ma and G170R-Mi/S81L-Ma variants in stably transformed CHO-GO cells. Twenty-four hours after seeding cells were fixed and coloured as follows: (**A**) anti-AGT (green) and anti-peroxisomal proteins (red) and (**B**) anti-FLAG (green) and anti-peroxisomal proteins (red). Nuclei were stained with Dapi (blue). Below is shown the RGB profile plotted along the line drawn in the merged image. Merge and single-channel images come from a single z-plane. Scale bar: 10 μm.

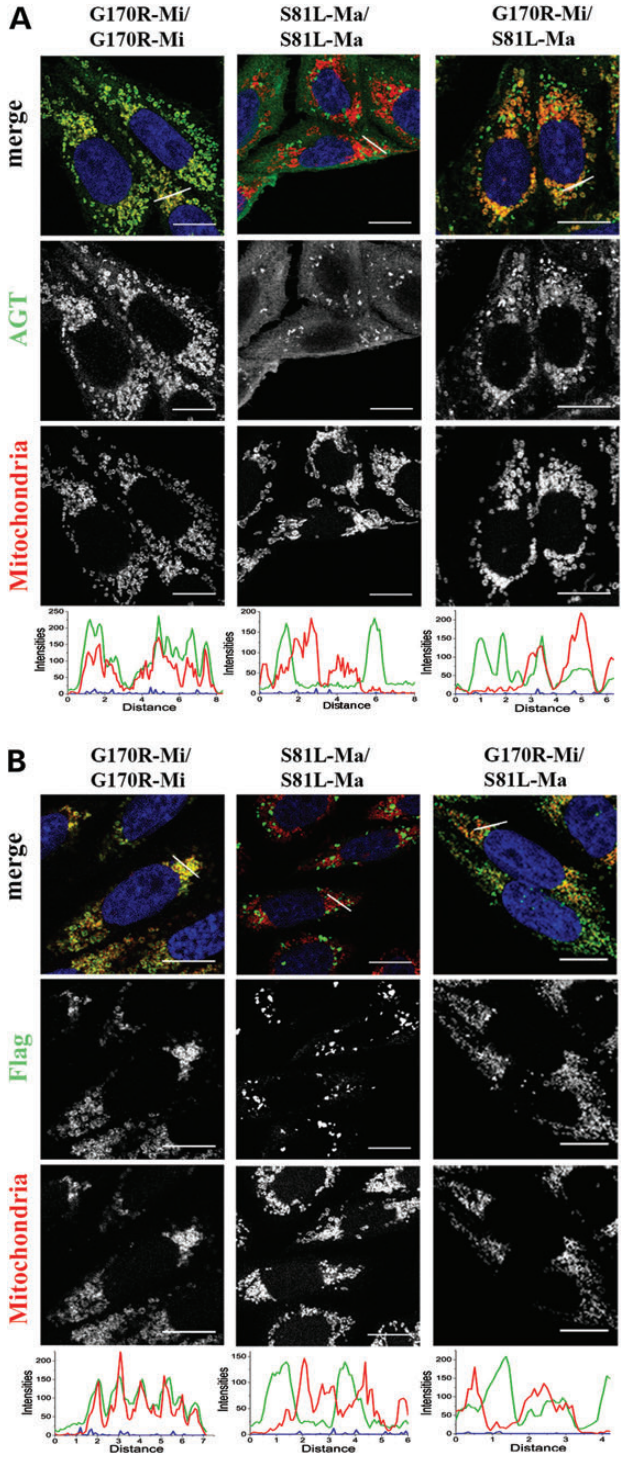

Figure 5. Subcellular distribution of G170R-Mi/G170R-Mi, S81L-Ma/S81L-Ma and G170R-Mi/S81L-Ma variants in stably transformed CHO-GO cells. Twenty-four hours after seeding cells were fixed and coloured as follows: (**A**) anti-AGT (green) and MitoTracker (red) and (**B**) anti-FLAG (green) and MitoTracker (red). Nuclei were stained with Dapi (blue). Below is shown the RGB profile plotted along the line drawn in the merged image. Merge and single-channel images come from a single z-plane. Scale bar: 10 μm.

intensity of the same pixel in two channels. It is generally accepted that only values of >0.5 are indicative of a meaningful colocalization (26). As expected, the localization of AGT-Ma/AGT-Ma,

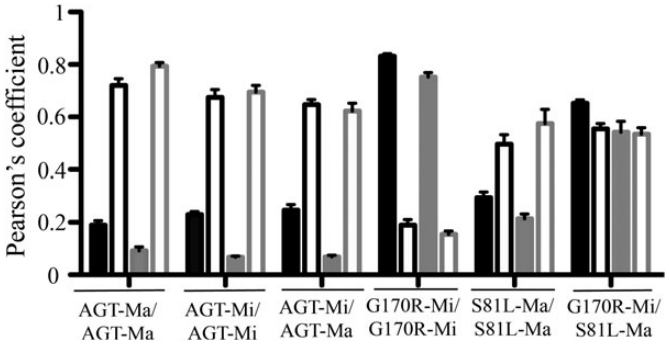

Figure 6. Pearson's coefficients for the subcellular distribution of the analysed AGT variants in stably transformed CHO-GO cells. The histogram bars represent the Pearson's coefficient calculated for the colocalization of: AGT and mitochondria (solid black), AGT and peroxisomes (outlined black), AGT-FLAG and mitochondria (solid grey), AGT-FLAG and peroxisomes (outlined grey). The results are given as means (± S.E.M.) of several images; at least 30 individual cells were analysed for each coefficient.

AGT-Mi/AGT-Mi and AGT-Mi/AGT-Ma was entirely peroxisomal (Supplementary Material, Figs S2 and S3), whereas that of G170R-Mi/G170R-Mi was entirely mitochondrial (Figs 5 and 6). Although S81L-Ma showed a significant peroxisomal localization, a portion of the protein is present in the cell cytosol (Fig. 6). Cross-linking and size-exclusion chromatography experiments of lysates of cells expressing this variant allowed us to exclude that the cytosolic localization was due to the formation of cytosolic aggregates not compatible with the peroxisomal import. Nevertheless, considering that the S81L-Ma homodimer is present in the cell mainly as apoenzyme, it is possible to hypothesize that the S81L mutation induces a conformational change on apoAGT causing the slowing down of the peroxisomal import. Indeed, the purified S81L-Ma apovariant showed with respect to apoAGT-Ma: (i) a slightly lower intrinsic fluorescence emission intensity, (ii) a near-UV CD spectrum characterized by an identical signal at 291 nm and by a completely lost signal at 284 nm and (iii) a 3-fold increased ANS emission fluorescence intensity (Supplementary Material, Fig. S4). We tried to favour the peroxisomal import by culturing the cells expressing the S81L-Ma/S81L-Ma in the presence of 100 μM pyridoxine to favour holoenzyme formation. However, only a partial reduction of the cytosolic amount of the protein could be observed.

Interestingly, the quantitative analysis of the distribution of AGT in cells expressing the G170R-Mi/S81L-Ma construct showed a significant peroxisomal localization as highlighted by staining with both the anti-AGT and the anti-FLAG antibody (Pearson coefficient of 0.55 and 0.53 for the colocalization of the peroxisomal marker with anti-AGT or anti-FLAG, respectively) (Fig. 6). It is worth to point out that cells expressing the G170R-Mi/S81L-Ma construct will produce S81L-Ma/S81L-Ma homodimers, G170R-Mi/G170R-Mi homodimers and G170R-Mi/S81L-Ma heterodimers. However, since the FLAG epitope in the construct is associated with the G170R-Mi moiety, the staining with the anti-FLAG antibody will only label G170R-Mi/G170R-Mi homodimers (known to be targeted to mitochondria) and G170R-Mi/S81L-Ma heterodimers. Therefore, the detection of the FLAG signal in the peroxisomes not only confirms the formation in an appreciable amount of the G170R-Mi/S81L-Ma heterodimers but also indicates their localization into peroxisomes.

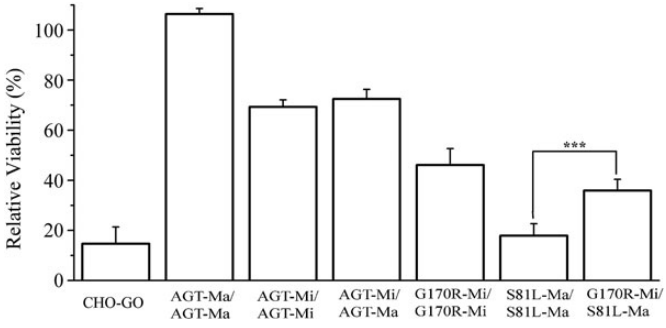

Figure 7. Glycolate cytotoxicity assay of CHO-GO cells expressing the AGT variants. The histogram is representative of the cell viability after 24 h of treatment with 250 μM glycolate expressed as percentage of untreated control. Bar graphs represent the mean ± SD. $^{***}P < 0.001$.

S81L and G170R mutations in homozygous and heterozygous conditions: effect on the AGT functionality

A glycolate-toxicity assay was used to assess the AGT functionality in the analysed clones. CHO-GO cells were treated with 250 μM glycolate for 24 h to allow the formation of peroxisomal glyoxylate by GO. Since glyoxylate induces cell death, the ability to survive in the presence of glycolate is a direct measure of the ability to detoxify peroxisomal glyoxylate. As shown in Figure 7, the protection against glycolate toxicity of AGT-Ma/AGT-Ma, AGT-Mi/AGT-Mi and AGT-Mi/AGT-Ma was 70–100% that of untreated cells. The G170R mutation reduced by about 50% the protection afforded by AGT-Mi/AGT-Mi, whereas the S81L mutation reduced by about 80% the protection afforded by AGT-Ma/AGT-Ma. Finally, the cell line expressing both variants has a viability equal within experimental error to that of cells expressing only the G170R-Mi variant. Thus, the amount of AGT able to detoxify glyoxylate in cells expressing both S81L-Ma and G170R-Mi is equal to that of cells expressing only G170R-Mi and higher than that of cells expressing S81L-Ma. This finding along with the coenzyme binding affinity and the subcellular localization of the heterodimer is relevant for its functionality.

DISCUSSION

In rare recessive diseases, many patients are compound heterozygous. Thus, their enzymatic phenotype results from the combination of the effect(s) of each single mutation when heteromeric protein forms are generated. Positive, negative or no IC effects are usually observed at the clinical level. These effects have been also investigated at the molecular level for few diseases such as phenylketonuria, argininosuccinate lyase deficiency and hypogonadotropic hypogonadism (27–29). These studies have been performed by looking to either the '*in vitro*' catalytic properties of the heteromeric proteins or the specific activity upon coexpression of the two variants in yeast and bacterial systems. Up to now, the correlation between the enzymatic and the clinical phenotype of PH1 compound heterozygous patients has never been investigated, although they represent a large percentage of PH1 patients.

In this work, for the first time, clinical, biochemical and cell biology data have been collected with the aim of understanding the effects of the S81L mutation on the major allele and the G170R on the minor allele under homozygous and heterozygous conditions. Our investigation was not limited to the AGT activity of the purified recombinant forms of S81L-Ma, G170R-Mi and S81L-Ma/G170R-Mi and to the specific activity upon expression or coexpression of the S81L and G170R variants in CHO cells but was extended to their expression level, coenzyme binding affinity, subcellular localization and functionality. This broad spectrum analysis resulted to be useful considering the multiplicity of the molecular mechanisms accounting for AGT deficiency. The results gave new significant insights into the PH1 mechanism, as we report the molecular basis of the pathogenicity of the S81L mutation on the major allele and the interplay between this mutation and the G170R mutation on the minor allele. When expressed individually, the S81L-Ma and G170R-Mi variants show distinct features. As already reported and confirmed in this study, when only G170R-Mi allele is expressed, AGT retains catalytic activity and PLP binding affinity, but it is almost completely redirected to mitochondria (12,15,17,18,24,25). On the other hand, we here report that when the S81L-Ma allele (lacking the putative MTS) is expressed, AGT shows a decreased catalytic activity, is almost completely present in the apo-form and is mainly peroxisomal. Thus, while the pathogenicity of the G170R mutation is related to AGT mistargeting, that of the S81L mutation is linked to the reduction of PLP binding affinity. What happens upon coexpression of both alleles? A pool of monomeric species with either the G170R mutation on the minor allele or the S81L mutation on the major allele should be virtually present in the cytosol. In theory, three different dimeric species, homodimers G170R-Mi, homodimers S81L-Ma and heterodimers G170R-Mi/S81L-Ma would be generated from the combination of the two coexpressed monomers. We were able to recreate the naturally occurring mutations S81L and G170R in AGT identified in compound heterozygous patient and to isolate and characterize the heterodimer in the purified recombinant form. This allowed us to establish that it exhibits a considerable k_{cat} value and, in agreement with its $K_{D(PLP)}$ value, it is present in the cell mainly in the holo-form. More importantly, it shows a peroxisomal localization. The peroxisome-to-mitochondrion mistargeting of AGT in PH1 is due to the combined effects of (i) the generation of an MTS resulting from the P11L polymorphism and (ii) the presence of monomeric AGT. Since in the heterodimer G170R-Mi/S81L-Ma, only the first condition occurs, even if limited to one subunit, its peroxisomal localization is not surprising. It can be also speculated that in cells expressing both S81L-Ma and G170R-Mi, the rate of the formation of the heterodimer is faster than that of the import of G170R-Mi monomers in mitochondria. Moreover, although cells expressing both G170R-Mi and S81L-Ma show a reduced expression level, they display an ability to detoxify glyoxylate greater than that of cells expressing homodimer S81L-Ma and equal to those expressing homodimers G170R-Mi. In the first case, this could be interpreted on the basis of the significant amount of protein present in the holo-form. In the second case, the detoxification ability could be ascribed to the proper subcellular localization of the heterodimer.

Altogether, these results indicate that the resulting hybrid protein has catalytic parameters not significantly different from those obtained theoretically by averaging the homodimeric counterparts, and a reduced expression level in the cellular system. However, the PLP binding affinity, the subcellular localization and the ability to detoxify glyoxylate make the

heterodimer more functional than the homodimeric counterparts. This implies that the association between the G170R and S81L monomers leads to a global positive IC between these mutations. On these bases, it can be speculated that compound heterozygous patients for the S81L mutation on the major allele and the G170R mutation on the minor allele could have a milder phenotype than homozygous S81L patients. In this regard, although it is not possible to drawn definitive conclusions only from two patients, the clinical data reported in this study appear to agree with our biochemical data. Indeed, the G170R/S81L compound heterozygous patient had a late onset of ESRD compared with the one functionally hemizygous for the S81L mutation who only expresses the S81L-Ma variant.

This work constitutes a valid example of an approach useful to understand the enzymatic phenotype in compound heterozygous PH1 patients, with potential applications to the study of the interaction between other pathogenic mutations. In fact, it should be emphasized that the use of different experimental approaches has been crucial to shed light on the molecular mechanisms of IC effects between the S81L and the G170R mutation. Besides providing a better knowledge of the disease pathogenesis, the results obtained could allow to develop proper therapeutic treatments, as the hybrid protein could have defects different from those of the parental enzymes.

MATERIALS AND METHODS

Materials

PLP, L-alanine, glyoxylate, pyruvate, rabbit muscle L-lactic dehydrogenase and mouse anti-FLAG antibody were purchased from Sigma-Aldrich. All other chemicals were of the highest purity available. CHO-GO cells, the rabbit polyclonal anti-AGT human, the anti-AGT-Ma and the guinea-pig anti-peroxisomal protein antibodies were kindly provided by Prof C.J. Danpure of the University College London, UK. Oligonucleotides were purchased from MWG Biotech.

Plasmids construction

To obtain the cDNA encoding the AGT-glutathione S-transferase (AGT-GST) fusion protein, the human AGT cDNA cloned in a pTrcHis2A prokaryotic expression vector (pAGThis) (6) was provided of a 5′ NcoI restriction site, a 3′ thrombin cleavage site and a 3′ BamHI restriction site by three sequential PCR amplifications using the forward primer AGTGSTfwd and the reverse primers AGTGSTrevA, AGTGSTrevB and AGTGSTrevC (Supplementary Material, Table S1). The GST cDNA was amplified from the pGEX-4T vector and provided of a 5′ BamHI restriction site and a 3′ EcoRI restriction site using the forward primer GSTfwd and the reverse primer GSTrev (Supplementary Material, Table S1). The two amplification products were digested with the BamHI restriction enzyme and ligated to obtain the AGT-GST fusion protein cDNA. To construct the plasmid pAGT-GST, the AGT-GST cDNA was subcloned into the pET28a vector using the NcoI and EcoRI restriction sites.

To generate the pAGTFLAG-Ma plasmid, the sequence (GAT TACAAGGATGACGATGACAAG) encoding for the FLAG tag (DYKDDDDK) was introduced at position 762 into the AGT coding sequence by means of site-directed insertion mutagenesis using the pAGThis construct as template, the insertion primers AGTFLAG1 and AGTFLAG2 (Supplementary Material, Table S1) and their complements.

Each construct was confirmed to be free of mutations by DNA sequencing.

Site-directed mutagenesis

Site-directed mutagenesis was performed by the QuikChange II site-directed mutagenesis kit (Stratagene) using the pAGThis-Ma (9) the pAGTFLAG-Ma and the pAGT-GST constructs as templates and the primers reported in Supplementary Material, Table S1.

Construction of pIRES vectors

The pIRES vector is a bicistronic plasmid that allows to express two genes in one transcript in mammalian cells. pIRES vectors encoding two copies of the AGT cDNA in different combinations (Fig. 1) were constructed by two subcloning phases. In the first phase, the cDNA encoding for AGTFLAG-Ma, AGTFLAG-Mi, AGTFLAG-S81L-Ma and AGTFLAG-G170RMa, obtained by site-directed mutagenesis from the pAGTFLAG-Ma construct, were subcloned in the first polycloning site using the primers pIres1fw and pIres1rev (Supplementary Material, Table S1) and the restriction enzymes NheI and EcoRI. In the second phase, the cDNA encoding for AGT-Ma, AGT-Mi, AGT-S81L-Ma and AGT-G170R-Mi were subcloned in the second polycloning site using the primers pIres2fw and pIres2rev (Supplementary Material, Table S1) and the restriction enzymes XbaI and NotI. Each construct was confirmed to be free of mutations by DNA sequencing.

Cell culture, selection and lysis

CHO-GO cells were cultured at 37°C under O_2/CO_2 (19 : 1) in Ham's F12 Glutamax medium (Invitrogen) supplemented with foetal bovine serum (10% v/v), penicillin (100 units/ml), streptomycin (100 μg/ml) and zeocin (0.4 mg/ml). Cells were transfected using the Turbofect^{TM} Transfection Reagent (Thermo-Fisher). After 24 h, G-418 (1.25 mg/ml) was added as selective agent and cells were left to grow for 48 h. To generate monoclonal stably transformed cell lines, the antibiotic-resistant transformants were seeded at limiting dilution of 10 cells/ml in 96-well plates in selective medium and incubated until single colonies started growing. Clones (at least 12 for each construct) were then growth and screened for exogenous gene expression by IFM and western blot. Cells were trypsinized, harvested and lysed in phosphate-buffered saline (PBS), pH 7.2, plus protease inhibitors (Complete Mini, Roche), by five freeze/thaw cycles followed by addition of DNAse (100 units/ml) at room temperature for 45 min. The whole cell extract was then centrifuged at 29,200*g* for 10 min at 4°C to obtain the soluble cellular lysate. Protein concentration was determined using the Bradford protein assay.

Enzymatic activity assays

For the measurement of AGT activity, 90 μg of cell lysate were incubated with 0.5 M L-alanine and 10 mM glyoxylate at 25°C in 100 mM potassium phosphate buffer (KP), pH 7.4, in the

presence or in the absence of 200 μM PLP. In order to obtain a detectable signal of pyruvate in the linear phase of the kinetics, the reaction time was set to 20 min for cells expressing the AGT-Ma/AGT-Ma, AGT-Mi/AGT-Ma and AGT-Mi/AGT-Mi constructs, and to 60 min for cells expressing the other constructs. The reactions were stopped by adding TCA 10% (v/v), and pyruvate production was measured using a spectrophotometric assay coupled with lactate dehydrogenase as previously described (6).

The kinetic parameters for the overall transamination of the pair L-alanine/glyoxylate of normal and mutant AGT were determined by incubating the purified protein (0.1 μM) in the presence of 200 μM PLP in 100 mM KP at 25°C and by varying the substrate concentration at a fixed saturating cosubstrate concentration. Pyruvate formation was measured by the spectrophotometric assay already reported (6). Data were fitted to the Michaelis–Menten equation.

GO enzymatic activity was measured by incubating 10 μg of cell lysate with 4 mM glycolate in 100 mM KP, pH 7.4, previously oxygenated and equilibrated at 25°C. The reaction was stopped after 15 min by addition of 10% TCA, and the glyoxylate produced was detected by HPLC after 2,4 dinitro-phenilhydrazine derivatization (30).

Transcript analysis

The total mRNA content was extracted from cells using the RNAeasy kit (Qiagen) and analysed by real-time PCR as described in Supplementary Material.

Western blot and immunoprecipitation

Four micrograms of cell lysate were loaded per lane on a Mini-Protean TGX™ pre-cast gel (Biorad) along with the Precision plus protein Kaleidoscope™ (BioRad) molecular mass markers. Proteins were transferred on a nitrocellulose membrane by the iBlot device (Invitrogen), and the membrane was blocked in 5% milk solution in TBST (50 mM Tris–HCl, pH 7.5, 150 mM NaCl, 0.1% Tween 20) for 1 h at RT. For AGT detection, the membrane was incubated with polyclonal rabbit anti-AGT serum (dilution 1 : 6000), washed three times in TBST and then incubated with peroxidase-conjugated anti-rabbit IgG (dilution 1 : 10 000). Blotted proteins were detected with ECL™ (Millipore), using the ChemiDocXRS Imaging System (BioRad, Hercules, CA, USA). Densitometry analysis was performed using the software ImageJ. For immunoprecipitation, 300 μg of cell lysates were incubated overnight with 300 μl of PBS buffer supplemented with 3 μg of mouse anti-FLAG IgG. The solutions were then incubated with Protein-A-Sepharose for 1 h, and the protein–antibody complexes were recovered by centrifugation. Samples were washed three times with PBS and analysed by western blot using a rabbit anti-AGT-Ma antiserum (1 : 1000).

Glycolate-toxicity assay

The glycolate-toxicity assay was performed as previously reported (15). CHO-GO cells were seeded at 7.000 cells/well in a 96-well plate and incubated 24 h before inducing glyoxylate production by adding Hepes buffered glycolate, pH 7.0, at a final concentration of 250 μM. Cell viability was evaluated after further 24-h incubation using the crystal violet staining (Sigma–Aldrich). Briefly, cells were rinsed with PBS, incubated at room temperature for 5 min with 4% formaldehyde + 0.5% crystal violet solution to perform fixing and staining. Cells were then extensively washed with distilled water to remove the excess of dye and lysed with 1% SDS in PBS to allow crystal violet solubilization and quantification. The absorbance at 595 nm, which is proportional to the number of viable cells, was measured with a TECAN plate reader. Six replicates were performed for each assay condition. Statistical analysis was performed with GraphPad Prism Version 5.0 (GraphPad software, San Diego, CA, USA).

IFM

A total of 3×10^5 cells were grown for 24 h into a 13-mm glass coverslip on a 24-well plate. For the mitochondrial labelling, cells were vitally stained for 30 min with MitoTracker Red (Molecular Probes). Cells were fixed in 4% (w/v) paraformaldehyde, permeabilized with 0.3% Triton X-100 in PBS and then blocked in 3% bovine serum albumin. For the immunolabelling, rabbit polyclonal anti-human AGT, anti-peroxisomal protein form guinea-pig and mouse monoclonal anti-FLAG were used as primary antibodies, and Alexa Fluor-conjugated antibodies (AF488 and AF555, Life technologies) were used as secondary antibodies. Nuclei were stained with DAPI (Molecular Probes), and the coverslips were mounted over slides in AF1 medium (Dako). The images were captured using a confocal laser-scanning fluorescence microscope Leica SP5 (Molecular Probes, Leica Microsystem) at 63× magnification. Pearson's coefficients were calculated using the ImageJ (http://rsb.info.nih.gov/ij/) JACoP plugin, and images were processed using Adobe Photoshop.

Expression and purification

The his-tagged AGT-Ma, AGT-Mi, G170R-Mi and S81L-Ma variants were expressed in *E. coli* and purified as already described (6). The S81L-Ma/G170R-Mi heterodimers were obtained by co-transforming *E. coli* BL21 (DE3) cells with vectors encoding the GST-tagged G170R-Mi variant and the his-tagged S81L-Ma variant and purified by a Ni-affinity chromatography followed by a GST-affinity chromatography. Details are given in Supplementary Material. The apo-form of each variant was prepared as previously described (6). The protein concentration in the AGT samples was determined using an extinction coefficient of 9.54 × 104/M/cm at 280 nm (6).

Determination of $K_{D(PLP)}$

The $K_{D(PLP)}$ values of heterodimeric S81L-Ma/G170R-Mi and those of homodimeric S81L-Ma were determined by measuring the quenching of the intrinsic fluorescence of the apoenzyme and the change of the CD signal at 430 nm, respectively, in the presence of PLP at varying concentrations, as described in Supplementary Material.

Spectroscopic measurements

Absorption, fluorescence and CD spectra were registered as described in Supplementary Material.

SUPPLEMENTARY MATERIAL

Supplementary Material is available at *HMG* online.

ACKNOWLEDGEMENTS

We gratefully acknowledge helpful suggestions by Prof M. De Marchi and Prof A. Amoroso of the University of Torino, and technical assistance by Silvia Bianconi.

Conflict of Interest statement. None declared.

FUNDING

This work was supported by Telethon Fundation (GGP10092 to C.B.V.). Funding to pay the Open Access publication charges for this article was provided by Telethon Foundation (Project GPP10092 to C.B.V.).

REFERENCES

1. Kopp, N. and Leumann, E. (1995) Changing pattern of primary hyperoxaluria in Switzerland. *Nephrol. Dial Transplant*, **10**, 2224–2227.
2. Cochat, P., Deloraine, A., Rotily, M., Olive, F., Liponski, I. and Deries, N. (1995) Epidemiology of primary hyperoxaluria type 1. Societe de Nephrologie and the Societe de Nephrologie Pediatrique. *Nephrol. Dial Transplant*, **10** Suppl 8, 3–7.
3. Danpure, C.J. and Rumsby, G. (2004) Molecular aetiology of primary hyperoxaluria and its implications for clinical management. *Expert. Rev. Mol. Med.*, **6**, 1–16.
4. Purdue, P.E., Lumb, M.J., Allsop, J. and Danpure, C.J. (1991) An intronic duplication in the alanine: glyoxylate aminotransferase gene facilitates identification of mutations in compound heterozygote patients with primary hyperoxaluria type 1. *Hum. Genet*, **87**, 394–396.
5. Zhang, X., Roe, S.M., Hou, Y., Bartlam, M., Rao, Z., Pearl, L.H. and Danpure, C.J. (2003) Crystal structure of alanine:glyoxylate aminotransferase and the relationship between genotype and enzymatic phenotype in primary hyperoxaluria type 1. *J. Mol. Biol.*, **331**, 643–652.
6. Cellini, B., Bertoldi, M., Montioli, R., Paiardini, A. and Borri Voltattorni, C. (2007) Human wild-type alanine:glyoxylate aminotransferase and its naturally occurring G82E variant: functional properties and physiological implications. *Biochem. J.*, **408**, 39–50.
7. Oppici, E., Fodor, K., Paiardini, A., Williams, C., Voltattorni, C.B., Wilmanns, M. and Cellini, B. (2013) Crystal structure of the S187F variant of human liver alanine: aminotransferase associated with primary hyperoxaluria type I and its functional implications. *Proteins*, **81**, 1457–1465.
8. Oppici, E., Montioli, R., Lorenzetto, A., Bianconi, S., Borri Voltattorni, C. and Cellini, B. (2012) Biochemical analyses are instrumental in identifying the impact of mutations on holo and/or apo-forms and on the region(s) of alanine:glyoxylate aminotransferase variants associated with primary hyperoxaluria type I. *Mol. Genet Metab.*, **105**, 132–140.
9. Lumb, M.J. and Danpure, C.J. (2000) Functional synergism between the most common polymorphism in human alanine:glyoxylate aminotransferase and four of the most common disease-causing mutations. *J. Biol. Chem.*, **275**, 36415–36422.
10. Cellini, B., Montioli, R., Paiardini, A., Lorenzetto, A. and Voltattorni, C.B. (2009) Molecular Insight into the Synergism between the minor allele of human liver peroxisomal alanine:glyoxylate aminotransferase and the F152I mutation. *J. Biol. Chem.*, **284**, 8349–8358.
11. Cellini, B., Montioli, R., Paiardini, A., Lorenzetto, A., Maset, F., Bellini, T., Oppici, E. and Voltattorni, C.B. (2010) Molecular defects of the glycine 41 variants of alanine glyoxylate aminotransferase associated with primary hyperoxaluria type I. *Proc. Natl. Acad. Sci. USA*, **107**, 2896–2901.
12. Mesa-Torres, N., Fabelo-Rosa, I., Riverol, D., Yunta, C., Albert, A., Salido, E. and Pey, A.L. (2013) The role of protein denaturation energetics and molecular chaperones in the aggregation and mistargeting of mutants causing primary hyperoxaluria type I. *PLoS One*, **8**, e71963.
13. Cellini, B., Oppici, E., Paiardini, A. and Montioli, R. (2012) Molecular insights into primary hyperoxaluria type 1 pathogenesis. *Front Biosci.*, **17**, 621–634.
14. Coulter-Mackie, M.B. and Lian, Q. (2006) Consequences of missense mutations for dimerization and turnover of alanine:glyoxylate aminotransferase: study of a spectrum of mutations. *Mol. Genet. Metab.*, **89**, 349–359.
15. Fargue, S., Lewin, J., Rumsby, G. and Danpure, C.J. (2013) Four of the most common mutations in primary hyperoxaluria type 1 unmask the cryptic mitochondrial targeting sequence of alanine:glyoxylate aminotransferase encoded by the polymorphic minor allele. *J. Biol. Chem.*, **288**, 2475–2484.
16. Oppici, E., Roncador, A., Montioli, R., Bianconi, S. and Cellini, B. (2013) Gly161 mutations associated with Primary Hyperoxaluria Type I induce the cytosolic aggregation and the intracellular degradation of the apo-form of alanine:glyoxylate aminotransferase. *Biochim. Biophys. Acta.*, **1832**, 2277–2288.
17. Cellini, B., Lorenzetto, A., Montioli, R., Oppici, E. and Voltattorni, C.B. (2010) Human liver peroxisomal alanine:glyoxylate aminotransferase: different stability under chemical stress of the major allele, the minor allele, and its pathogenic G170R variant. *Biochimie*, **92**, 1801–1811.
18. Danpure, C.J., Purdue, P.E., Fryer, P., Griffiths, S., Allsop, J., Lumb, M.J., Guttridge, K.M., Jennings, P.R., Scheinman, J.I., Mauer, S.M. *et al.* (1993) Enzymological and mutational analysis of a complex primary hyperoxaluria type 1 phenotype involving alanine:glyoxylate aminotransferase peroxisome-to-mitochondrion mistargeting and intraperoxisomal aggregation. *Am. J. Hum. Genet.*, **53**, 417–432.
19. Williams, E.L., Acquaviva, C., Amoroso, A., Chevalier, F., Coulter-Mackie, M., Monico, C.G., Giachino, D., Owen, T., Robbiano, A., Salido, E. *et al.* (2009) Primary hyperoxaluria type 1: update and additional mutation analysis of the AGXT gene. *Hum. Mutat.*, **30**, 910–917.
20. Robbiano, A., Frecer, V., Miertus, J., Zadro, C., Ulivi, S., Bevilacqua, E., Mandrile, G., De Marchi, M., Miertus, S. and Amoroso, A. (2010) Modeling the effect of 3 missense AGXT mutations on dimerization of the AGT enzyme in primary hyperoxaluria type 1. *J. Nephrol.*, **23**, 667–676.
21. Behnam, J.T., Williams, E.L., Brink, S., Rumsby, G. and Danpure, C.J. (2006) Reconstruction of human hepatocyte glyoxylate metabolic pathways in stably transformed Chinese-hamster ovary cells. *Biochem. J.*, **394**, 409–416.
22. Kubota, H. (2009) Quality control against misfolded proteins in the cytosol: a network for cell survival. *J. Biochem.*, **146**, 609–616.
23. Fargue, S., Rumsby, G. and Danpure, C.J. (2013) Multiple mechanisms of action of pyridoxine in primary hyperoxaluria type 1. *Biochim. Biophys. Acta.*, **1832**, 1776–1783.
24. Pey, A.L., Salido, E. and Sanchez-Ruiz, J.M. (2011) Role of low native state kinetic stability and interaction of partially unfolded states with molecular chaperones in the mitochondrial protein mistargeting associated with primary hyperoxaluria. *Amino Acids*, **41**, 1233–1245.
25. Danpure, C.J. (2006) Primary hyperoxaluria type 1: AGT mistargeting highlights the fundamental differences between the peroxisomal and mitochondrial protein import pathways. *Biochim. Biophys. Acta.*, **1763**, 1776–1784.
26. Bolte, S. and Cordelieres, F.P. (2006) A guided tour into subcellular colocalization analysis in light microscopy. *J. Microsc.*, **224**, 213–232.
27. Leandro, J., Leandro, P. and Flatmark, T. (2011) Heterotetrameric forms of human phenylalanine hydroxylase: co-expression of wild-type and mutant forms in a bicistronic system. *Biochim. Biophys. Acta.*, **1812**, 602–612.
28. Leanos-Miranda, A., Ulloa-Aguirre, A., Janovick, J.A. and Conn, P.M. (2005) In vitro coexpression and pharmacological rescue of mutant gonadotropin-releasing hormone receptors causing hypogonadotropic hypogonadism in humans expressing compound heterozygous alleles. *J. Clin. Endocrinol. Metab.*, **90**, 3001–3008.
29. Howell, P.L., Turner, M.A., Christodoulou, J., Walker, D.C., Craig, H.J., Simard, L.R., Ploder, L. and McInnes, R.R. (1998) Intragenic complementation at the argininosuccinate lyase locus: reconstruction of the active site. *J. Inherit. Metab. Dis.*, **21** Suppl 1, 72–85.
30. Cellini, B., Bertoldi, M. and Borri Voltattorni, C. (2003) Treponema denticola cystalysin catalyzes beta-desulfination of L-cysteine sulfinic acid and beta-decarboxylation of L-aspartate and oxalacetate. *FEBS Lett.*, **554**, 306–310.